

Novel ytterbium and thulium lasers based on the monoclinic $\text{KLu}(\text{WO}_4)_2$ crystalline host

Valentin Petrov,^{a),*} Xavier Mateos,^{a)} Simon Rivier,^{a)} Oscar Silvestre,^{b)} Magdalena Aguilo,^{b)}
Rosa Sole,^{b)} Maria Cinta Pujol,^{b)} Junhai Liu,^{a)} Uwe Griebner,^{a)} Francesc Diaz^{b)}

^{a)}Max-Born-Institute for Nonlinear Optics and Ultrafast Spectroscopy,
2A Max-Born-Str., D-12489 Berlin, Germany;

^{b)}Group of Física i Cristal·lografia de Materials (FiCMA), Universitat Rovira i Virgili,
Campus Sescelades c/ Marcel·lí Domingo, s/n, E-43007 Tarragona, Spain

ABSTRACT

High-quality crystals of $\text{KLu}(\text{WO}_4)_2$, shortly KLuW, were grown with sizes sufficient for characterization of the thermo-mechanical and optical properties, and substantial progress was achieved in the field of spectroscopy and laser operation with Yb^{3+} - and Tm^{3+} -doping. We review the properties of flux grown KLuW, the Yb^{3+} and Tm^{3+} spectroscopy, and present laser results obtained in several operational regimes both with Ti:sapphire and direct diode laser pumping using InGaAs and AlGaAs diodes near 980 and 800 nm, respectively. The slope efficiencies with respect to the absorbed pump power achieved with continuous-wave (CW) bulk and epitaxial Yb:KLuW lasers under Ti:sapphire laser pumping were $\approx 57\%$ and $\approx 66\%$, respectively. Output powers as high as 3.28 W were obtained with diode pumping in a simple two-mirror cavity where the slope efficiency with respect to the incident pump power reached $\approx 78\%$. Passively Q-switched laser operation of bulk Yb:KLuW was realized with a Cr:YAG saturable absorber resulting in oscillation at ≈ 1031 nm with a repetition rate of 28 kHz and simultaneous Raman conversion to ≈ 1138 nm with maximum energies of 32.4 and 14.4 μJ , respectively. The corresponding pulse durations were 1.41 and 0.71 ns. Passive mode-locking by a semiconductor saturable absorber mirror (SESAM) resulted in bandwidth-limited pulses with duration of 81 fs (1046 nm, 95 MHz) and 114 fs (1030 nm, 101 MHz) for bulk and epitaxial Yb:KLuW lasers, respectively. Slope efficiency as high as 69% with respect to the absorbed power and an output power of 4 W at 1950 nm were achieved with a diode-pumped Tm:KLuW laser. The tunability of this laser, under Ti:sapphire laser pumping, extended from 1800 to 1987 nm. An epitaxial Tm:KLuW laser provided slope efficiency as high as 64% and a tuning range from 1894 to 2039 nm when pumped by a Ti:sapphire laser.

Keywords: rare earth solid state lasers; monoclinic double tungstates

1. INTRODUCTION

The main advantages of the monoclinic potassium double tungstates as laser hosts are the very high values of the absorption and emission cross sections of the rare-earth dopants, partly due to the strong anisotropy of these biaxial crystals, and the possibility to dope them with high concentration of the active ions without substantial fluorescence quenching. Information on the synthesis, crystal structure and some thermal properties of monoclinic KLuW appeared for the first time in 1968.¹ Many properties of KLuW like the thermal conductivity, hardness, optical transparency, and refractive index are very similar to those of the isostructural $\text{KY}(\text{WO}_4)_2$ (KYW).² Single crystals of KLuW were used to analyze the infrared and Raman spectra³ and efficient high-order Stokes and anti-Stokes stimulated Raman scattering (SRS) in the visible and near-infrared was observed for the two SRS-active modes at 907 and 757 cm^{-1} .² Laser emission of Er:KLuW was demonstrated for the 0.85, 1.74 and 2.81 μm transitions,⁴ the luminescence properties and laser

* E-mail: petrov@mbi-berlin.de

operation of Ho:KLuW for the 2.08 and 2.94 μm lines were also studied,^{5,6,7} but most of the spectroscopic and laser works were devoted to Nd:KLuW,^{7,8,9,10} where the 1.07 and 1.35 μm lines were investigated and CW generation at 1070.2 nm was achieved at room temperature with diode pumping.¹⁰ Recently, some additional activities were focused on the growth, spectroscopy and diode-pumped laser operation of Nd:KLuW.^{11,12,13} It is known that KNd(WO₄)₂ has a different, tetragonal scheelite structure, and Nd-doping of KLuW is limited to about 3 at % because stresses and cracks occur.^{8,14} The KLuW host seems actually predestined for doping with Yb because of the close ionic radii and masses of Yb and Lu, and the close lattice parameters of the isostructural KLuW and KYb(WO₄)₂ (KYbW).¹⁵ This allows high Yb-doping levels with low defect formation probability and epitaxial growth of highly absorbing films with best quality of the interface. Moreover, the Yb-dopant affects only weakly the thermal conductivity of the host. The next most suitable dopant for KLuW seems Tm. In that case the two hosts KLuW and KYW have similar deviations from KTm(WO₄)₂. Here we will review the growth, structure, and physical properties of KLuW, the spectroscopy of Yb³⁺ and Tm³⁺ in KLuW, and the laser results obtained by us with bulk and epitaxial Yb:KLuW and Tm:KLuW crystals (see Table I). Note that more recently, KLuW was also doped with Sm¹⁶ and Dy,¹⁷ as well as co-doped with Er:Yb, by the present authors and in Ref.17, and with Yb:Tm,¹⁸ but lasing has not been demonstrated in such crystals, yet.

TABLE I
Laser operation demonstrated with rare-earth doped KLuW.

Ln ³⁺	doping ^f [at. %]	polarization ^o	transition	wavelength [nm]	pump	remarks*	reference (year)
Nd	3	$\perp a$	$^4F_{3/2} \rightarrow ^4I_{13/2}$	1348.2	Xe-lamp	pulsed	Ref. 7 (1979)
Nd	2	$\perp a', \perp c$	$^4F_{3/2} \rightarrow ^4I_{13/2}$	1353.3, 1355	Xe-lamp	pulsed	Ref. 8 (1983)
Nd	2	$\perp b$	$^4F_{3/2} \rightarrow ^4I_{13/2}$	1355			
Nd	3	$\perp a$	$^4F_{3/2} \rightarrow ^4I_{11/2}$	1071.4	Xe-lamp	pulsed	Ref. 7 (1979)
Nd	2	$\perp a'$	$^4F_{3/2} \rightarrow ^4I_{11/2}$	1072.1	Xe-lamp	77 and 300 K, pulsed	Ref. 8 (1983)
Nd	2	$\perp b, \perp c$	$^4F_{3/2} \rightarrow ^4I_{11/2}$	1070.1, 1070.2			
Nd	~5	NA	$^4F_{3/2} \rightarrow ^4I_{11/2}$	1070.1	pyro-lamp	quasi-CW	Ref. 9 (1983)
Nd	3	$\perp b$	$^4F_{3/2} \rightarrow ^4I_{11/2}$	1070.2	diode laser	quasi-CW, CW	Ref. 10 (1992)
Nd	3	$\perp b$	$^4F_{3/2} \rightarrow ^4I_{11/2}$	1073	diode laser	CW	Ref. 13 (2005)
Er	3, 5, 25	$\perp b, \perp c$	$^4I_{11/2} \rightarrow ^4I_{13/2}$	2809.2	Xe-lamp	pulsed	Ref. 4 (1979)
Er	3, 5	$\perp b$	$^4S_{3/2} \rightarrow ^4I_{9/2}$	1738.3			
Er	5	$\perp b$	$^4S_{3/2} \rightarrow ^4I_{13/2}$	~850			
Ho	3	$\perp c$	$^5I_7 \rightarrow ^5I_8$	2079	Xe-lamp	110 K, pulsed	Ref. 6 (1981)
Ho	3	$\perp b$	$^5I_6 \rightarrow ^5I_7$	2944.5	Xe-lamp	pulsed	Ref. 7 (1979)
Yb	5, 10	//N _m	$^3F_{5/2} \rightarrow ^3F_{7/2}$	1033.3-1051.3	Ti:sapphire	CW	Ref. 19,20 (2004)
Yb	5	//N _m	$^3F_{5/2} \rightarrow ^3F_{7/2}$	1041-1047	diode laser	CW	Ref. 19,20 (2004)
Yb	5	//N _m	$^3F_{5/2} \rightarrow ^3F_{7/2}$	1039.5-1052.4	diode laser	CW	Ref. 21 (2005)
Yb	5	//N _p	$^3F_{5/2} \rightarrow ^3F_{7/2}$	1046	Ti:sapphire	CW	Ref. 22 (2005)
Yb	5	//N _m	$^3F_{5/2} \rightarrow ^3F_{7/2}$ 1st Stokes	1030.6 1137.6	diode laser	Q-switched + self-Raman laser	Ref. 21 (2005)
Yb	5	//N _m	$^3F_{5/2} \rightarrow ^3F_{7/2}$	1046	Ti:sapphire	M-L, fs	Ref. 22 (2005)
Yb	5	//N _p	$^3F_{5/2} \rightarrow ^3F_{7/2}$	1043, 1049 1053	Ti:sapphire diode laser	M-L, ps & fs, M-L, fs	Ref. 22 (2005)
Yb	10	//N _m	$^3F_{5/2} \rightarrow ^3F_{7/2}$	1026-1040 1030	Ti:sapphire diode laser	epitaxy, CW	Ref. 23 (2005)
Yb	50	//N _m	$^3F_{5/2} \rightarrow ^3F_{7/2}$	1032, 1046.1	Ti:sapphire	quasi-CW, CW	Ref. 24 (2006)
Yb	10	//N _m	$^3F_{5/2} \rightarrow ^3F_{7/2}$	1030	Ti:sapphire	epitaxy, M-L, ps & fs	Ref. 25 (2005)
Tm	3	//N _m	$^3F_4 \rightarrow ^3H_6$	1943-1975	diode laser	CW	Ref. 26,27 (2006)
Tm	3, 5	//N _m	$^3F_4 \rightarrow ^3H_6$	1917-1951 1809-1983	Ti:sapphire	CW CW-tunable	Ref. 27 (2006)
Tm	3	//N _p	$^3F_4 \rightarrow ^3H_6$	1907-1942 1800-1987	Ti:sapphire	CW CW-tunable	
Tm	5	//N _m	$^3F_4 \rightarrow ^3H_6$	1960-1967 1894-2039	Ti:sapphire	epitaxy, CW CW-tunable	Ref. 28 (2007)

^fdoping level in the solution; the data on the segregation coefficient of Nd in Refs. 11,13 is contradictory; ^othe crystallographic a' axis ($I2/c$ space group) is at $\approx 44.7^\circ$ from the a -axis ($C2/c$ space group); *M-L: mode-locked; if not mentioned, the temperature is 300 K.

2. GROWTH AND CRYSTAL STRUCTURE OF BULK AND EPITAXIAL KLuW

KLuW exhibits a polymorphic transformation just below its melting point.²⁹ Thus, the low-temperature, monoclinic form can be grown only from high-temperature solutions. We use the top-seeded solution growth (TSSG) slow-cooling method with a cylindrical vertical furnace as described elsewhere.³⁰ The composition is about 12/88 mol % solute/solvent ($K_2W_2O_7$). This is the standard solvent used for KLuW, with the basic advantages being the absence of foreign ions and the low melting temperature;³⁰ another possibility is K_2WO_4 .^{1,11,12} The crystals are grown in Pt crucibles using K_2CO_3 , WO_3 , and Ln_2O_3 ($Ln=Lu, Yb, Tm$) as starting materials, with 99.9% purity. A seed along the *b*-crystallographic axis is attached to a Pt holder rotating at 40 rpm. The temperature gradient in the solution is about 1 K/cm in the vertical and radial directions with the bottom and walls being hotter. The growth occurs as a result of supersaturation when cooling below the saturation temperature which depends on the flux composition and slightly increases with the doping level. The cooling interval is about 20 K, and the cooling rate varies between 0.1 and 0.3 K/h, depending on the crystal size and the doping level. Finally, the grown crystals are removed slowly from the solution and cooled at a rate of 15-25 K/h, slightly above the surface. Typical sizes and weights are about one cm³ and several grams (see Fig. 1). The segregation coefficients, both for Yb and Tm doping, are close to or above unity.^{18,19,20,26,27} The crystalline forms which are developed are {110}, {-111}, {010} and {310}, Fig. 1a. Further information on the growth conditions, mechanisms, morphology and habits of bulk KLuW can be found in the corresponding literature.^{31,32,33,34,35}

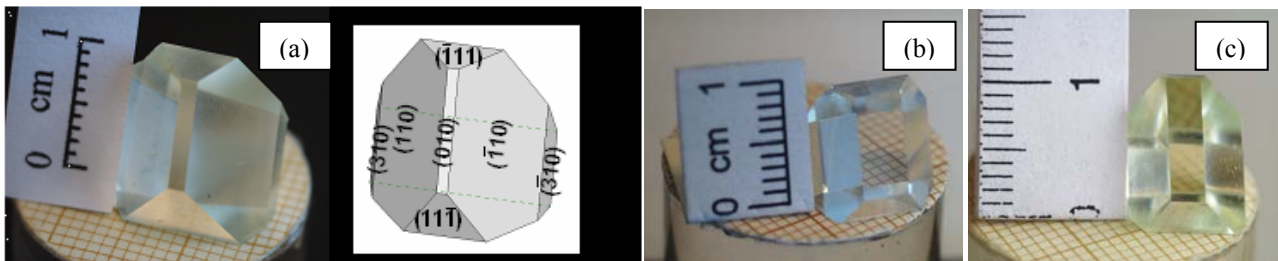


Fig. 1. Undoped (a), 5 at % Yb-doped (b), and 3 at % Tm-doped (c) crystals of KLuW grown by the TSSG method.

The low-temperature monoclinic phase of KLuW has the structure of KYW.¹ The unit cell parameters we determined in the $C2/c=C_{2h}^6$ space group by single crystal X-ray diffraction (XRD) are included in Table II; these data are close to previous measurements using powder XRD,^{14,15} or more recent ones performed on single crystals.³⁶ The unit cell parameters increase with the doping level, both for Yb³¹ and Tm.³⁷

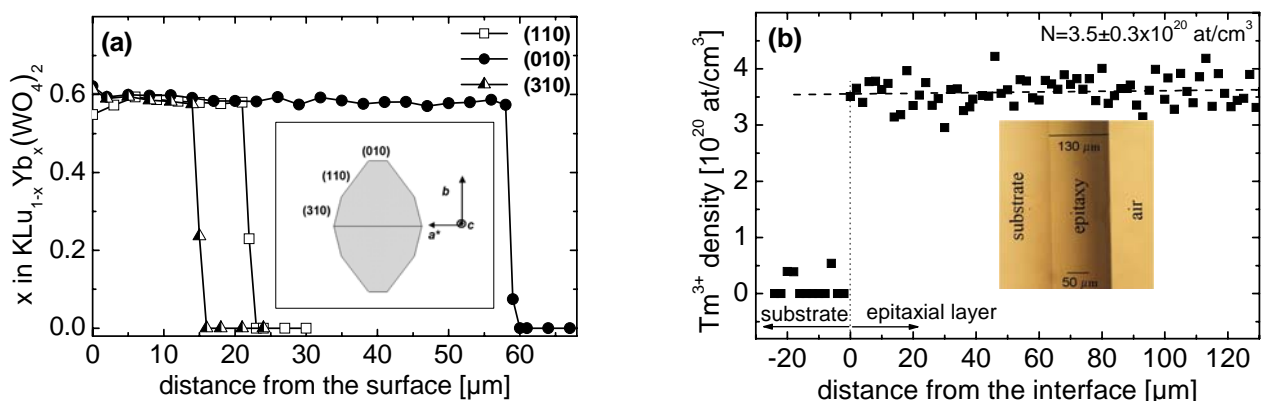


Fig. 2. Measured Yb-density profile for a Yb:KLuW/KLuW composite on three different faces (a) and Tm-density distribution for the (010) face of a Tm:KLuW/KLuW composite (b). The insets show the faces studied (a) and a microscope image of the layer region (b).

The production of thin doped layers is important in the case of highly absorbing materials, especially for the use in simplified (less pump passes) versions of the thin disk laser concept, the power scalability of which is inversely proportional to the crystal thickness, but also in general for a better overlap with the pump beam in the case of diode pumping. The latter is relevant also to waveguide structures which can be fabricated by different techniques for refractive index manipulation: e.g. oxygen ion implantation was recently used for planar waveguide structures based on Yb:KLuW.³⁸ The monoclinic double tungstates are very promising for thin film laser designs just because of the high doping levels and interaction cross sections. Thus, e.g. the stoichiometric KYbW which exhibits only weak fluorescence quenching has an absorption length of only 13.3 μm for pumping at 981 nm with polarization $E//N_m$.³⁹

We applied liquid phase epitaxy (LPE) for production of thin Yb- and Tm-doped single layers on passive KLuW substrates. KLuW is obviously the best choice for Yb-doped monoclinic composites because the lattice mismatch with respect to KYbW (0.33% on the average) is minimum.²³ The growth technique was basically the same but the special furnace had a wide zone of uniform temperature to ensure almost vanishing temperature gradient. Also, the solvent part was increased to 93-95 mol % for better control of the growth rate according to the solubility curves.^{23,28,32} The epitaxial growth took place for several hours at a temperature 1-6 K below the saturation temperature.^{28,32} The doping level was 5-50 at % for Yb³² and 5 at % for Tm.²⁸ Also for the epitaxial growth, the segregation coefficients of Yb and Tm were close to or larger than unity. There was no appreciable diffusion of the dopant from the layer into the substrate (Fig. 2). It turned out that the (010) face tends to grow faster and this face had also the highest quality of the layer (Fig. 2). More information on the morphology, growth habits and characteristics of the layers obtained can be found elsewhere.³²

3. PROPERTIES OF KLuW

The information previously available on the properties of KLuW was limited to the average refractive indices at 0.7 μm (≈ 2.08)² and 0.9...1.4 μm (≈ 1.9)⁸, the transparency (0.3...5.5 μm for a thickness of 1 mm),^{2,8} the average thermal conductivity (≈ 3 W/m/K),² and the hardness in the Moh's scale (4.5-5).² We have collected in Table II the results obtained since the "rediscovery" of KLuW as a laser host in 2004, see Table I. The transparency and the wavelength dependence of the refractive indices of KLuW, together with the obtained Sellmeier expansions, are shown in Fig. 3.^{20,31}

TABLE II
Some physical properties of the monoclinic KLuW crystal host.

passive laser host	KLu(WO ₄) ₂ or KLuW	Ref.
temperature of polymorphic transformation / melting [K]	1313 ⁺ / 1328 ⁺ , 1330	40
crystal structure (space group – point group)	monoclinic centrosymmetric ($C2/c \equiv C_{2h}^6 - 2/m$)	31
site symmetry / coordination number / Lu ³⁺ ionic radius	$C_2 / 8 / 1.117 \text{ \AA}$	31
lattice constants	$a=10.576(7) \text{ \AA}$, $b=10.214(7) \text{ \AA}$, $c=7.487(2) \text{ \AA}$, $\beta=130.68(4)^\circ$, $Z=4$	31
cell volume and density	$613.3(6) \text{ \AA}^3$ and 7.686 g/cm^3	31
cation density / minimum Lu-Lu separation	$6.52 \times 10^{21} \text{ cm}^{-3} / 4.045(3) \text{ \AA}$	31
transparency range (1 cm ⁻¹ level for 1 mm thickness)	365-5110 nm	20
refractive index @ 1 μm	$n_p=1.995$, $n_m=2.030$, $n_g=2.084$	31
optical ellipsoid orientation (632.8 nm)	$N_p//b$, $\angle(a, N_m)=58.7^\circ$, $\angle(c, N_g)=18.5^\circ$	31
angle between the two optic axes at 1064 nm	$2V_g=82.03^\circ$ (optically positive)	31
strongest phonon modes [cm ⁻¹]	908, 755	3 ^f
specific heat @ 90°C (826°C)	365 (701) J/kgK	40**
thermal conductivity coefficients κ @ 25°C (290°C) and orientation of the conductivity ellipsoid ($X_1X_2X_3$)	$\kappa_1=3.09(2.49) \text{ W/mK}$, $\kappa_2=2.55(2.05) \text{ W/mK}$, $\kappa_3=4.40(3.15) \text{ W/mK}$ $X_2//b$, $\angle(a, X_1)=6.34^\circ(1.94^\circ)$, $\angle(X_3, c)=34.4^\circ(38.8^\circ)$	40**
thermal expansion coefficients α [$10^{-6}/\text{K}$] and orientation of the thermal ellipsoid ($X_1X_2X_3$)	$\alpha_{11}=8.98(12.8)$, $\alpha_{22}=3.35(7.8)$, $\alpha_{33}=16.72(22.2)$ $X_2//b$, $\angle(a, X_1)=27.24^\circ(30.37^\circ)$, $\angle(X_3, c)=13.51^\circ(10.37^\circ)$	31* (41)**
microhardness numbers for planes \perp (axis)	VH=440(a*), 410 (b), 560(c) VH=393.5 KHN=366 (a), 417 (b), 489 (c)	31 11*** 40

⁺unpublished (present authors); ^finfrared and Raman spectra for 5% Yb-doped KLuW can be found in Ref. 42; *measurements by powder XRD of the cell parameters at 25-500°C; **measurements by a thermal dilatometer at 50-600°C (Ref. 41), other data for 5% Yb and 6% Tm co-doped KLuW can be found in Ref. 18; ***for 3% Nd-doped KLuW with unspecified orientation.

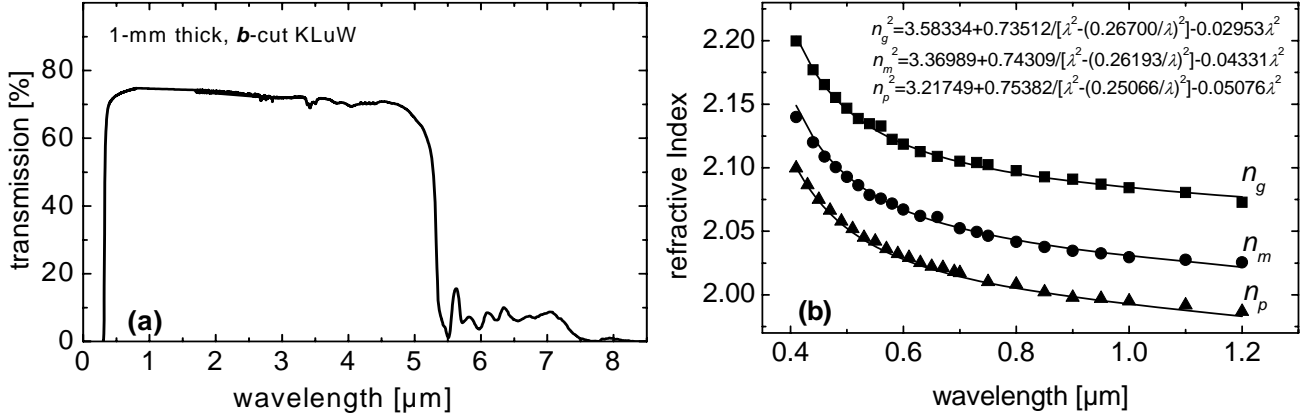


Fig. 3. Unpolarized transmission (a) and dispersion of the refractive indices (b) of undoped KLuW.

4. SPECTROSCOPY OF Yb- AND Tm-DOPED KLuW

The spectroscopic properties of bulk Yb:KLuW and Tm:KLuW are summarized in Fig. 4 and Table III. The useful polarizations are $E//N_m$ and $E//N_p$ because the cross sections for $E//N_g$ are very low. No difference was observed in the spectroscopy of thin Yb-doped epitaxial layers.³² The Stark splitting of the Yb and Tm levels can be found elsewhere.^{20,37}

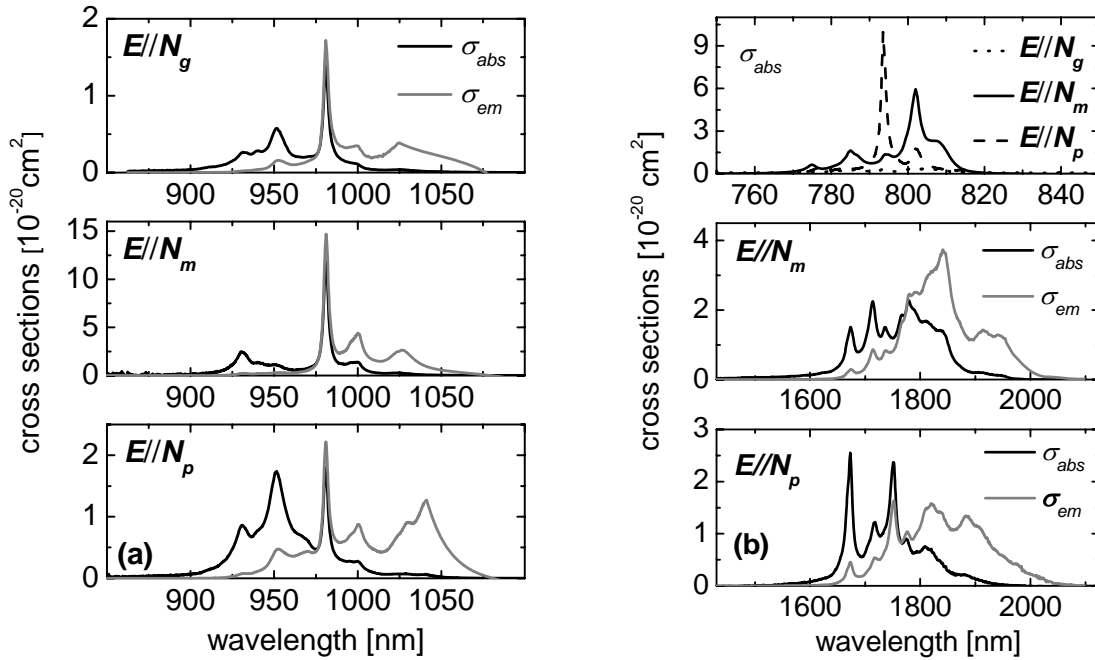


Fig. 4. Polarized measured absorption (black lines) and calculated emission (gray lines) cross-sections of Yb:KLuW (a). Polarized absorption cross sections of Tm:KLuW for the ${}^3H_6 \rightarrow {}^3H_4$ transition and absorption (black lines) and emission (gray lines) cross sections of Tm:KLuW for the ${}^3H_6 \leftrightarrow {}^3F_4$ transition and polarizations $E//N_m$ and $E//N_p$ (b).

TABLE III
Some spectroscopic properties of Yb- and Tm-doped KLuW (from Refs. 19, 20, 26, 27, 37).

spectral parameters	Yb:KLuW		Tm:KLuW	
	1.3-1.4 / 100%			
segregation coefficient / maximum doping level	1-1.2 / 20%			
lower laser level [cm^{-1}]	559	435	530	
thermal population @ 300 K [%]	4.22	7.64	1.94	
$^2F_{5/2}$ fluorescence lifetime [μs]	375 (0.5 at %), * 299 (5 at %)**		-	
calculated $^2F_{5/2}$ radiative lifetime [μs]	320		-	
3F_4 fluorescence lifetime [μs]	-		1340 (3 at %), ⁺ 900 (5 at %) ⁺	
absorption wavelength for $E//N_m$ and $E//N_p$ [nm]	981.1	980.9	802	793.5
absorption linewidth for $E//N_m$ and $E//N_p$ [nm]	3.6	4	4	1
σ_{abs} for $E//N_m$ and $E//N_p$ [10^{-20}cm^2]	11.8	1.8	5.95	9.96
laser (reference) wavelength λ_{ref} [nm]	1040		1950	
emission bandwidth (FWHM) [nm]	≈ 22	≈ 28	-	-
σ_{em} [10^{-20}cm^2] @ λ_{ref}	1.01	1.24	1.20	0.57
σ_{reabs} [10^{-20}cm^2] @ λ_{ref}	0.06	0.07	0.11	0.025

*bulk crystal, **pinhole method (unpublished), ⁺pinhole method.

5. BULK AND EPITAXIAL Yb-KLuW LASERS

The laser operation of the bulk and epitaxial samples was studied in three- or four-mirror cavities (Figs. 5a,b) with Ti:sapphire laser (1 nm linewidth) pumping or using a tapered diode laser (TDL) with 1 nm linewidth and $M^2 < 3$ for the slow axis. The uncoated crystals were positioned under Brewster angle which determines the laser polarization and the pump polarization was always in the same plane. A simple two-mirror cavity (Fig. 5c) was used for power scaling, pumping by an unpolarized fiber coupled diode module (116 μm core diameter, 0.2 NA) with $f=6.2$ mm micro-optics.

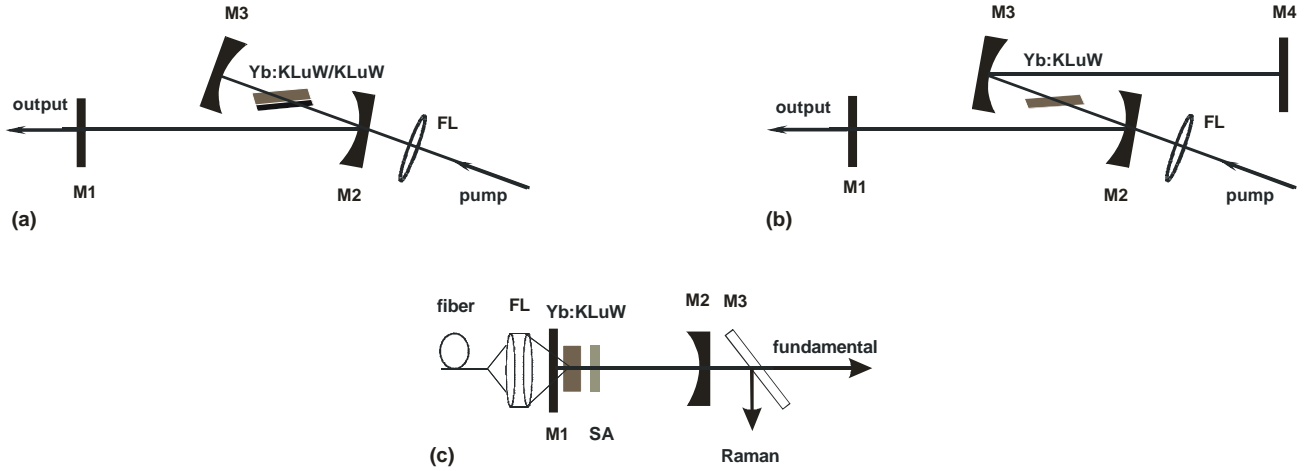


Fig. 5. Astigmatically compensated three- (a) and four- (b) mirror cavities for longitudinal pumping of the Yb:KLuW laser. In (a), the radii of curvatures, RC, of M3 and M2 are -5 and -10 cm, respectively; in (b) the folding mirrors (M2-M3) have RC=-10 cm; in both cases FL is a lens with $f=6.28$ cm. Hemispherical cavity for power scaling (c): The output coupler (M2) has a RC=-2.5 cm, SA denotes saturable absorber, and M3 is a dichroic mirror separating the fundamental and Raman radiation.

Using the Z-type cavity from Fig. 5b with Ti:sapphire laser pumping and without special cooling, the CW laser performance of a 5% Yb:KLuW (2.8 mm thick) sample and a 10% Yb:KLuW (2.2 mm thick) sample, both with $b(N_p)$ -cut, was very similar in terms of efficiency against absorbed pump power P_{abs} , Figs. 6a,b. There was only slight difference in the optimum pump (λ_p) and the oscillation (λ_L) wavelengths. This is an indication of the unaffected crystal

quality and upper level lifetime by the increased doping. The maximum output power for both crystals was $P_{out} \approx 1$ W ($T_{OC}=5\%$) for $P_{abs} \approx 2$ W which means an optical-to-optical efficiency of roughly 50%.

The imperfect overlap of the laser and pump modes in the case of TDL pumping resulted in increased thresholds and reduced slope efficiency η (Fig. 6c). The maximum $P_{out} = 170$ mW ($T_{OC}=5\%$) for $P_{abs} = 1.14$ W gives an optical-to-optical efficiency of 15%. The bleaching of the absorption in the case of Ti:sapphire laser pumping (pump waist ≈ 30 μ m), was suppressed when the laser was aligned as a result of the increased pump saturation intensity in the three-level Yb-system. In contrast, no bleaching was observed in the case of TDL pumping. The $E//N_p$ polarization was studied with an analogous 5% Yb:KLuW (3 mm thick) sample with N_m -cut. At $P_{abs} = 1.7$ W (Ti:sapphire laser pumping), $P_{out} = 750$ mW was obtained at 1046 nm for $T_{OC}=5\%$ ($\eta=54.2\%$) which is close to the 800 mW obtained for $E//N_m$ with the 5% doped b -cut sample (Fig. 6a). The thresholds with these two samples for $T_{OC}=5\%$ were 280 and 250 mW, respectively.

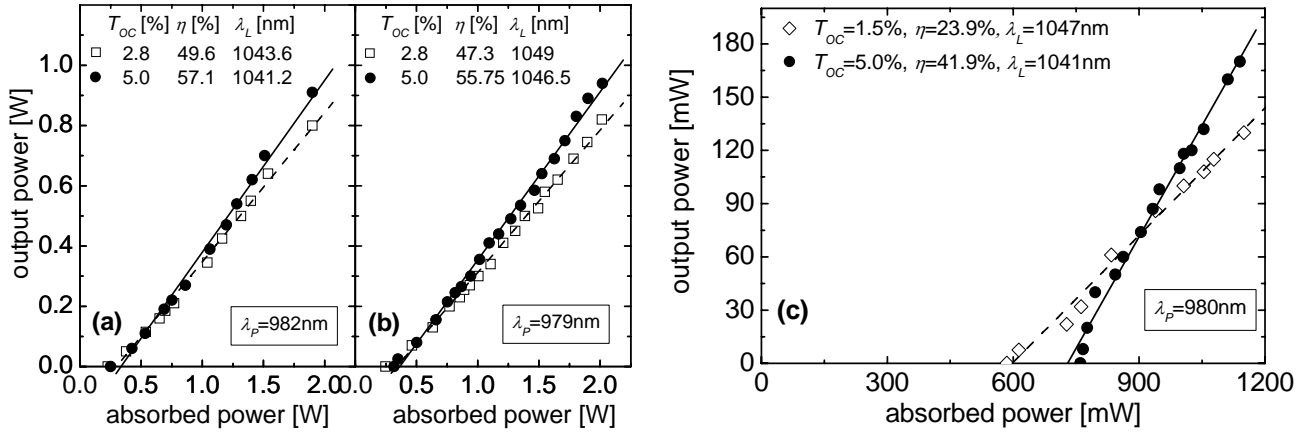


Fig. 6. Output power versus absorbed pump power of the Ti:sapphire laser pumped Yb:KLuW laser using the 140-cm long cavity from Fig. 5b with double pass pumping, through 80% retroreflection of the residual pump, for two different output couplers T_{OC} : 5% Yb-doping (a), and 10% Yb-doping (b). Input-output characteristics obtained with single pass TDL pumping of the same 5% Yb:KLuW sample in the same cavity from Fig. 5b (c). In all cases the pump and laser polarizations are $E//N_m$.

Power scaling was studied using a 3-mm thick, uncoated KLuW sample with 5% Yb-doping and b -cut, mounted in a water-cooled Cu-block, and placed in the two mirror cavity depicted in Fig. 5c. The most efficient CW laser operation with $T_{OC}=2\%$ (Fig. 7a) resulted in $P_{out}=3.28$ W for an incident pump power of 6.8 W. It was impossible to measure P_{abs} under lasing conditions in this compact cavity but the small signal absorption was 85-90%. The deviation from the linear dependence in Fig. 7a at low powers is related mainly to the changing (from 973 to 978 nm) multi-peaked pump spectrum while the absence of saturation at high powers indicates that further scaling should be possible.

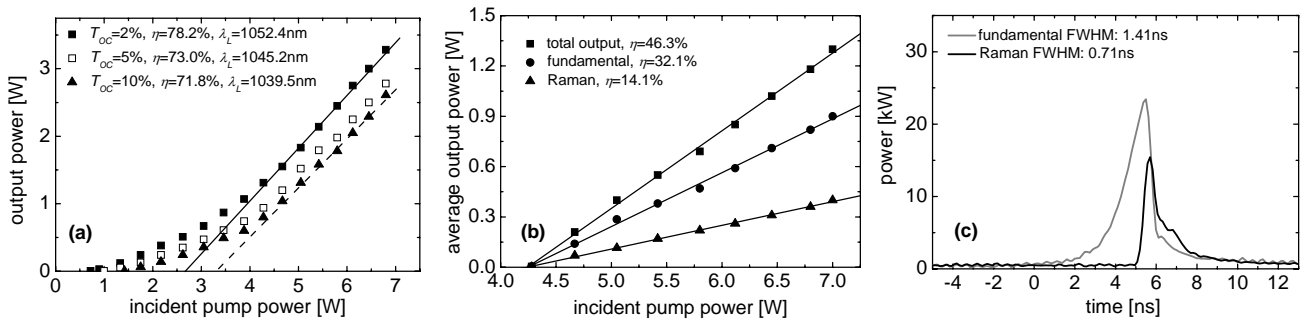


Fig. 7. Output power versus absorbed pump power of the CW Yb:KLuW laser pumped by an unpolarized fiber-coupled diode in the 2.5 cm long plano-concave cavity from Fig. 5c (a), average powers in the Q-switched regime (b), and temporal pulse profiles recorded for the fundamental and Raman radiation at a repetition rate of 28 kHz (c). In all cases the laser is naturally polarized in $E//N_m$.

By introducing a Cr^{4+} :YAG saturable absorber (a 1 mm thick AR-coated plate with 80% transmission) into the cavity (Fig. 5c), passively Q-switched laser operation was achieved. The most appropriate output coupler for this regime had a transmission of 10% at 1030 nm and $\approx 20\%$ at the Raman line. Slightly above the threshold (4.28 W of incident pump power), SRS occurred and the output spectrum consisted of the fundamental line at 1030.6 nm and the 1st Stokes line at 1137.6 nm. At the highest available pump power (7 W incident upon the crystal), the total average output power reached 1.3 W, with a Raman contribution of 0.4 W, Fig. 7b. The pulse repetition rate increased linearly from 6 kHz at threshold to 28 kHz at the highest pump level. The maximum energies of the fundamental and Raman pulses at 28 kHz were 32.4 and 14.4 μJ , respectively. Having in mind the measured pulse durations (Fig. 7c), the corresponding peak powers amount to 23 and 15.2 kW. The pulse-to-pulse fluctuations, both for the fundamental and the Raman radiation, were less than 5%. Also in the Q-switched regime, no saturation of the power dependence is observed (Fig. 7b).

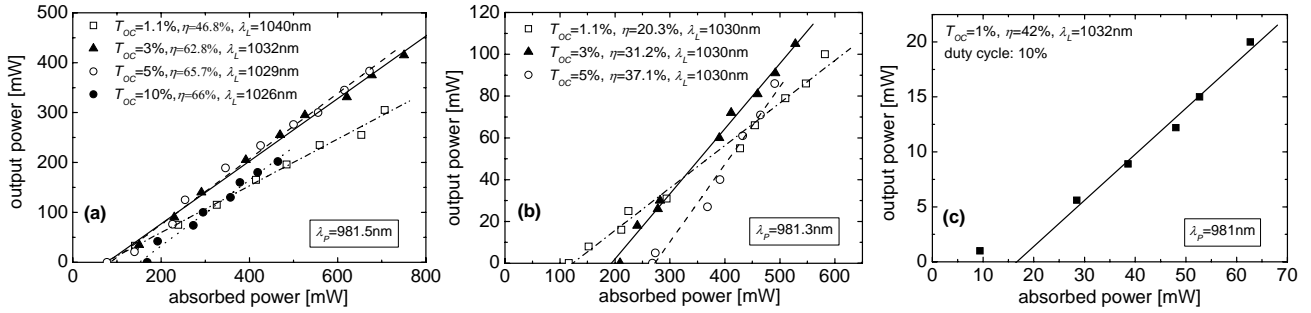


Fig. 8. Output power versus absorbed pump power for a 10% Yb:KLuW epitaxy pumped in the 67 cm long cavity from Fig. 5a by the Ti:sapphire laser (a), and by the TDL (b), and quasi-CW laser performance of a 50% Yb:KLuW epitaxy: average powers (c).

The CW laser experiments with an uncoated 10% Yb:KLuW epitaxial sample (a 100 μm layer grown on a 1.1 mm thick undoped substrate) were performed in the V-type cavity shown in Fig. 5a without special cooling. The maximum P_{out} achieved with 1.85 W of incident power from the Ti:sapphire pump laser in a single pass was 415 mW, for $T_{OC}=3\%$ (Fig. 8a), corresponding to an optical-to-optical efficiency of 55%. The increased efficiency, the roughly 4 times lower thresholds, and the shorter λ_L in comparison to bulk 10% Yb:KLuW are attributed to the reduced reabsorption. Recycling of the pump using another end mirror in Fig. 5a, it was possible to increase the output to 515 mW at 1030 nm. The low signal absorption of this epitaxy which was *b*-cut and oriented for $E//N_m$, was about 64%; it was bleached by the pump, but in both cases, Ti:sapphire and TDL pumping, the bleaching effect was almost compensated in the lasing state. The thresholds obtained with the TDL and the same set-up were also lower, 3 to 5 times with respect to the bulk Yb:KLuW, Fig. 8b. Here obviously the improved overlap plays a role, too. The maximum output power reached in this case, $P_{out}=105$ mW for $T_{OC}=3\%$, gives an optical-to-optical efficiency of 20%.

We tested also a 50% Yb:KLuW epitaxy which was cut for the same propagation and polarization directions but the doped layer was only 38 μm thick. However, linear dependence of the input-output characteristics was obtained only using a chopper. The maximum average P_{out} obtained was 20 mW for $P_{abs}\approx 63$ mW which gives an optical-to-optical efficiency of $\approx 32\%$. The average P_{out} obtained with the same $T_{OC}=1\%$ increased to 43 mW when double-pass pumping was applied. Although the absorption of this sample was quite optimum, strong thermal effects made it very difficult to achieve true CW operation. Pumping again in the absorption maximum, in a single pass, only 17 mW of average P_{out} at 1046.1 nm were obtained in this case for $P_{abs}=250$ mW, using a special $T_{OC}=0.1\%$ output coupler. For incident powers exceeding 400 mW the output quickly dropped to zero and even optical damage was observed above 500 mW. The extensive heating at high doping levels is attributed to impurities absorbing the laser and/or pump radiation which then relax non-radiatively. The influence of excitation migration to impurities can be ruled out because no substantial shortening of the fluorescence lifetime was observed for the 50% Yb-doped KLuW epitaxy.

The Z-shaped cavity used for mode-locking of the Yb:KLuW lasers is shown in Fig. 9. Two dispersion compensating prisms could be inserted in the arm with the output coupler. The SESAM was grown by the MOCVD-method and consisted of a bottom Bragg mirror comprising 25-pairs AlAs/GaAs quarterwave layers designed for a central wavelength of 1030 nm. The reflection band extended from 980 to 1070 nm. The 10-nm-thick InGaAs surface quantum well structure had a saturable loss of $\approx 1\%$ and a relaxation time < 5 ps.

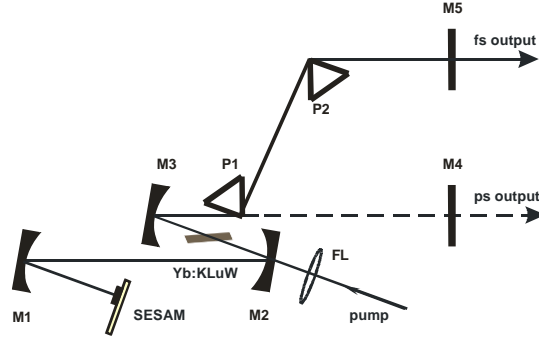


Fig. 9. Schematic of the astigmatically compensated cavity of the mode-locked Yb:KLuW laser. The folding mirrors (M1-M3) are with $RC=-10$ cm, P1 and P2 are SF10 prisms, and FL is a lens with $f=6.28$ cm.

The 2.8-mm thick crystal oriented for $E//N_m$ and the 3-mm thick crystal oriented for $E//N_p$, both with 5% Yb-doping, were first compared with Ti:sapphire laser pumping, without special cooling. Without intracavity prisms, the laser operated in the picosecond regime with a pulse repetition rate of 98 MHz. Pulses as short as 2.8 ps near 1043 nm were obtained for $E//N_p$ at a maximum average P_{out} of 540 mW ($T_{OC}=5\%$) corresponding to an optical-to-optical efficiency of 32%. The measured autocorrelation traces were fitted assuming a sech^2 -pulse shape. The 13 nm broad (FWHM) spectrum indicates that the pulse duration in the picosecond mode exceeds the Fourier limit by a factor of 30. The performance of the *b*-cut sample for $E//N_m$ was similar.

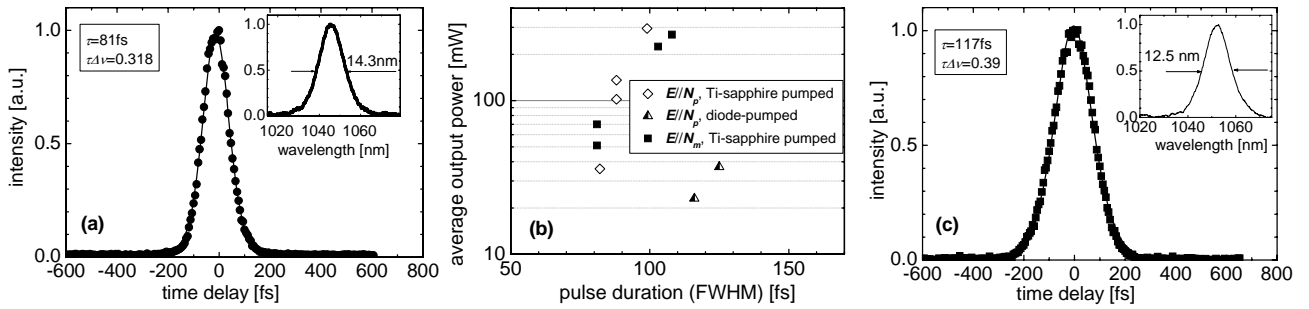


Fig. 10. Shortest pulses obtained from the Ti:sapphire laser pumped mode-locked bulk Yb:KLuW laser for $E//N_m$ (a), comparison of the laser performance for the two polarizations $E//N_m$ and $E//N_p$ (b), and shortest pulses obtained with TDL pumping for $E//N_p$ (c).

The two SF10 Brewster prisms introduced for femtosecond operation had a tip-to-tip separation of 38 cm. The resulting pulse repetition rate was 95 MHz. The FWHM of the shortest pulse obtained for $E//N_m$ was 81 fs (Fig. 10a), at an average $P_{out}=70$ mW ($T_{OC}=3\%$). The corresponding spectrum was centered at 1046 nm and had a FWHM of 14.3 nm (inset Fig. 10a). This results in a time-bandwidth product of 0.318 corresponding to transform-limited sech^2 -pulses. The results achieved for $E//N_m$ and $E//N_p$ are compared in Fig. 10b. Only minor differences can be seen, in accordance with the similar bandwidths of the calculated gain cross sections. In both crystal orientations mode-locking was achieved for $T_{OC}=1\dots5\%$. The shortest pulse duration obtained for $E//N_p$ was 83 fs at 1049 nm, for $P_{out}=36$ mW ($T_{OC}=1\%$). The output power increased to 295 mW for a pulse duration of 100 fs (Fig. 10b).

Using the TDL for pumping and the $E//N_p$ -oriented crystal, stable femtosecond mode-locking was achieved for $T_{OC}=1\dots3\%$. A maximum P_{out} of 56 mW was obtained in the mode-locked regime for $T_{OC}=3\%$ at an incident pump power of 1 W. The minimum pulse duration of 117 fs (FWHM) and the corresponding spectrum centered at 1053 nm (Fig. 10c) give a time-bandwidth product of 0.39.

Mode-locking with the 10% Yb:KLuW epitaxy was realized in the same cavity (Fig. 9) with Ti:sapphire laser pumping. In the picosecond regime, the laser operated at 100 MHz, the emission spectrum was centered at 1030 nm and the FWHM of the pulse was 1.8 ps (Fig. 11a). The input-output characteristics, below and above the mode-locking threshold, are shown in Fig. 11b. The maximum output power was $P_{out}=119$ mW with $T_{OC}=3\%$.

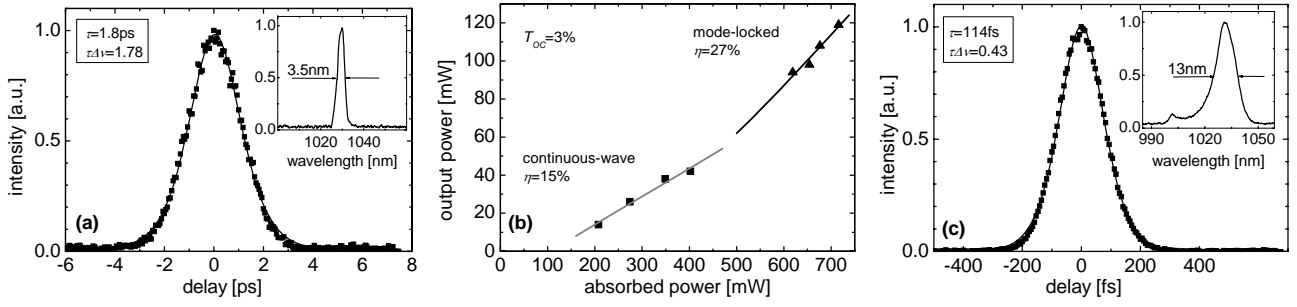


Fig. 11. Mode-locked performance of the epitaxial Yb:KLuW laser in the picosecond regime (a,b), and autocorrelation trace and spectrum in the femtosecond regime (c). In all cases the polarization is $E//N_m$.

The femtosecond regime was realized for $T_{OC}=1.1\%$ and a separation of 31 cm of the two intracavity prisms which resulted in a repetition rate of 101 MHz. Pulses as short as 114 fs (Fig. 11c) were generated at 1030 nm, with average $P_{out}=31$ mW for $P_{abs}=632$ mW. The time-bandwidth product was slightly above the Fourier limit. The lower limit for the pulse duration and the observed deviation from the transform-limitation seem related to the reflection characteristics of the folding mirrors which are restricted by the close separation between λ_P and λ_L . P_{out} increased to 94 mW using $T_{OC}=3\%$, again at $\lambda_L=1030$ nm, for $P_{abs}=671$ mW. The generated pulses had a FWHM of 200 fs in this case and were almost bandwidth-limited ($\tau\Delta\nu=0.32$).

6. BULK AND EPITAXIAL Tm:KLuW LASERS

The 90 cm long X-type cavity shown in Fig. 12a was used for pumping of Tm:KLuW by a Ti:sapphire laser (linewidth ≈ 0.2 nm). For power scaling, a single 50 W commercial bar with 19 emitters (linewidth ≈ 2 nm) and simple adapted beam shaping optics were used with the 5 cm long cavity shown in Fig. 12b. In the position of the crystal, the pump spot had a Gaussian waist of 37 μm (Ti:sapphire laser) and 62 μm (diode laser).

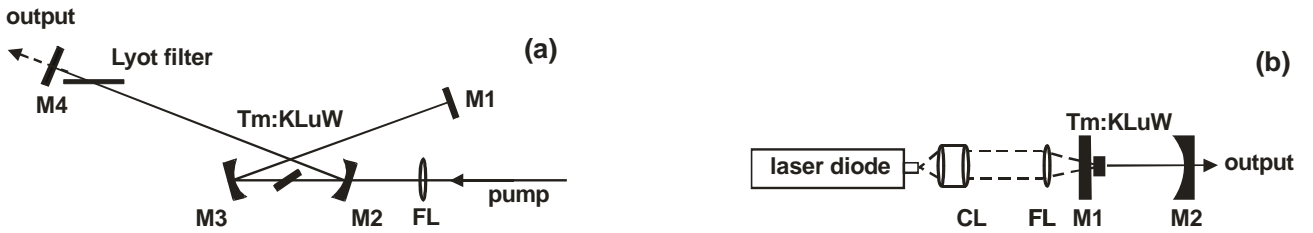


Fig. 12. Astigmatically compensated cavity of the tunable Tm:KLuW laser designed for Ti:sapphire laser pumping (a), and hemispherical cavity of the diode-pumped Tm:KLuW laser (b). In (a) the folding mirrors (M2-M3) are with $RC=-10$ cm and FL is a lens with $f=7$ cm. In (b) CL and FL are collimating and focusing lens systems with $f=3.4$ and 2 cm, respectively, and the output coupler (M2) is with $RC=-5$ cm.

Two bulk samples were available for pumping with the Ti:sapphire laser: The maximum P_{out} achieved with the 5% Tm:KLuW sample (*b*-cut, thickness: 2 mm) without cooling, for $E//N_m$ and $T_{OC}=3\%$, was 650 mW at $\lambda_L=1948$ nm ($\eta=60.5\%$). This sample absorbed 1.21 W of the incident 1.32 W at 802 nm. The threshold (P_{abs}) was 73 mW. The 3% Tm:KLuW sample (thickness: 2.92 mm) allowed to compare the two polarizations, $E//N_m$ and $E//N_p$, because it was N_g -cut (Fig. 13a,b). It was mounted in a Cu-block whose temperature was maintained at 10°C by circulating water. The maximum $P_{out}=1.4$ W for $P_{abs}=2.47$ W, achieved for $E//N_m$ and $T_{OC}=5\%$, corresponds to an optical-to-optical efficiency of 56.7% at a threshold of $P_{abs}=125$ mW. For polarization $E//N_p$, the maximum P_{out} achieved was slightly lower (1.28 W for $T_{OC}=10\%$ and $P_{abs}=2.61$ W). The absorption of the sample for $E//N_m$ under lasing conditions was 85-90% depending on the output coupler and for $E//N_p$ it was about 95%. While the absorption for $E//N_p$ obviously dropped when changing λ_P to 802 nm, a wavelength interesting for (unpolarized) diode-pumping, the thresholds and efficiencies in terms of P_{abs} remained basically the same.

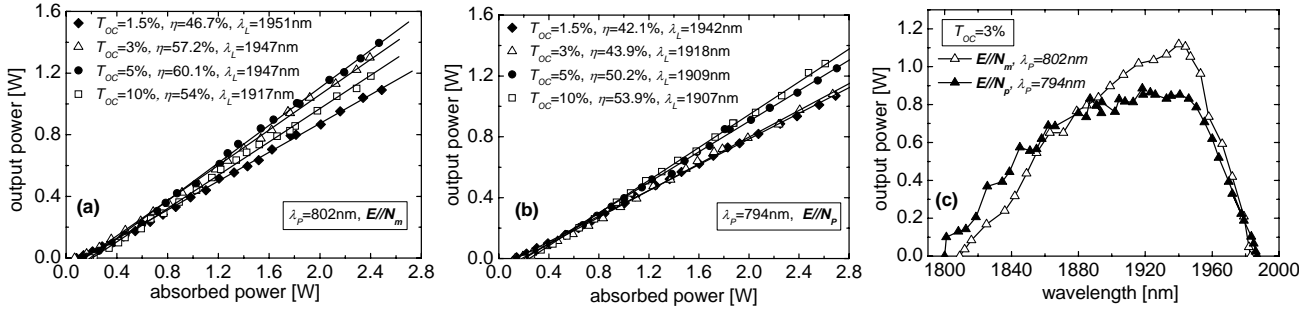


Fig. 13. Input-output laser characteristics of the 3% Tm:KLuW sample for $E//N_m$ (a) and $E//N_p$ (b): In both cases the maximum incident pump power was 2.83 W. Output power versus wavelength of the tunable 3% Tm:KLuW laser for $P_{abs}=2.4$ W (c).

Tuning was studied with the 3% Tm:KLuW sample introducing a 3-mm thick quartz plate (optical axis at 60° to the surface) into the long arm of the cavity (Fig. 12a). The overall tuning range extended from 1800 to 1987 nm (Fig. 13c), with FWHMs of 110 nm ($E//N_m$) and 128 nm ($E//N_p$). In the shorter wavelength limit the gain for $E//N_p$ was higher.

The unpolarized diode laser pump source used with the cavity from Fig. 12b had a maximum power of 14 W (measured behind the collimating lens) at 802 nm for an operating temperature of 25°C . At 20 W the wavelength was already 804.5 nm. The same 3% Tm:KLuW sample was mounted in a Cu-holder and room temperature was maintained by water cooling. The maximum P_{out} achieved with $T_{OC}=3\%$ was 4 W at $\lambda_L=1950$ nm for an incident pump power of 15 W (Fig. 14a). The slope efficiency calculated with respect to P_{abs} amounted to $\eta=69\%$ and the maximum optical-to-optical efficiency reached 47%. Obviously the cross-relaxation is very efficient in Tm:KLuW even at a doping level of 3% since without this process the upper limit for η would be 41%. The linear dependence of the output power is reached at higher pump levels in Fig. 14a. Such a behavior is typical for three-level laser systems in the presence of reabsorption losses which increase with the crystal temperature. At high power levels the M^2 parameter (deviation from the fundamental Gaussian mode) was ≈ 2.2 .

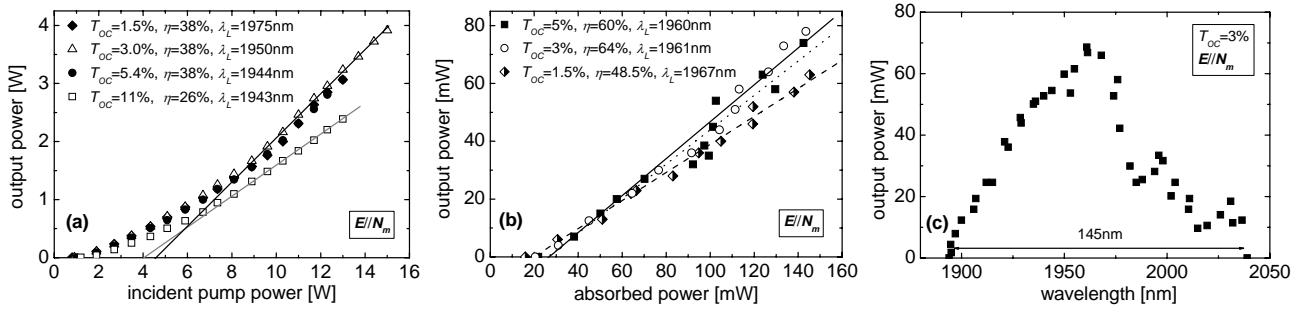


Fig. 14. Input-output characteristics of the diode-pumped bulk Tm:KLuW laser (a), and the Ti:sapphire laser pumped Tm:KLuW epitaxy (b), and tuning of the epitaxial Tm:KLuW laser using an intracavity Lyot filter (c). The polarization in (a) is naturally selected.

The 5% Tm:KLuW epitaxial sample with a total thickness of 1.7 mm (substrate+130 μm thick doped layer), mounted in a Cu-block without active cooling, was studied in the same cavity from Fig. 12a with Ti:sapphire laser pumping. It was b -cut and the only possible polarization was $E//N_m$ (Fig. 14b). A maximum $P_{out}=78$ mW was obtained for $T_{OC}=3\%$. In this case, the pump power incident on the crystal was 1.23 W but the absorbed power measured under lasing conditions was only 144 mW. The results, in terms of slope efficiency, are very similar to those obtained with the bulk 5% Tm:KLuW. The output power obtained with the epitaxial sample was relatively low due to the low absorption under lasing conditions. While the calculated small signal absorption was of the order of 24%, the absorption measured without lasing was strongly bleached and dropped to about 4%. In the three-level system of Tm, the intracavity intensity modifies the saturation intensity for the pump and the actual absorption increased to about 15% (almost constant with the incident power) but this was still too low. The low absorption lead also to the substantially lower thresholds ($P_{abs}=16$ -22 mW depending on T_{OC}) in comparison to the bulk Tm:KLuW.

Insertion of the same Lyot filter allowed to obtain almost continuous tuning from 1894 up to 2039 nm (Fig. 14c). This means a total spectral range of 145 nm with a single output coupler, the FWHM is roughly 60 nm. This result compares very well with the performance of the bulk Tm:KLuW laser, although the exact tuning range depends on the doping level, the absorption coefficient, and the output coupler.

7. CONCLUSION

Since Lu is the closest ion to Yb in the lanthanide series of the periodic table, KLuW is the most suitable host belonging to the family of the monoclinic double tungstates for Yb-doping. Besides the fact that the incorporation of Yb is easier and up to 100% doping can be achieved without affecting the quality of the grown crystals, the small lattice mismatch between KLuW and KYbW is advantageous for epitaxial growth of thin doped layers on undoped substrates. Furthermore, it is expected that the thermal conductivity of KLuW is least affected by Yb-doping. KLuW exhibits also good mechanical properties facilitating high quality polishing and coating. The next closest active ion (radius, mass) to Lu is Tm: hence KLuW is also a promising host for this dopant. In contrast to Yb, the Tm-ion exhibits quenching at high doping even in the monoclinic double tungstates. Nevertheless, the other attractive features of the double tungstates, highest absorption and emission cross sections and relatively broad bandwidths, suitable both for tuning and mode-locking, remain. Both Yb and Tm exhibit in KLuW absorption peaks which match very well the emission spectra of commercial InGaAs and AlGaAs diode lasers. This is an important prerequisite for power scaling of such lasers.

Most of the properties of the passive host crystal KLuW are now known. The spectroscopy of Yb and Tm is also well studied. We achieved extremely high slope efficiencies for CW laser operation, both with Yb- and Tm-doped KLuW crystals, which approach the theoretical limits. In both cases diode pumping allowed to obtain multiwatt output powers. While the slope efficiencies with epitaxial composites were also rather high, there are still problems to be solved related to nonradiative, heat producing processes at high doping levels. Higher purity of the raw materials used for the flux growth process will be an important factor for the advance in this direction. Once the problem with absorbing impurities in the KLuW host is solved, it can be expected that such epitaxies could lead to a breakthrough in the thin disk laser concept reducing it to a single pump pass with extremely efficient one-dimensional heat removal.

We demonstrated impressive tunability of the Tm-lasers, both bulk and epitaxial, in the 2- μm spectral range. The gain bandwidths are quite large, both for Yb and Tm, which means that passive mode-locking can produce sub-100 fs light pulses. Since SESAMs are at present available only for the 1 μm spectral range, we were able to demonstrate this only for Yb:KLuW lasers, both bulk and epitaxial. The host KLuW is also attractive for SRS. This can be realized in a single cavity using the same doped crystal and passive Q-switching. We achieved this regime with Yb:KLuW and a saturable absorber producing sub-ns pulses at the 1st Stokes.

The future work will be focused on better heat removal through special geometries of the active elements (thin slabs or disks) as well as implementation of reflective and antireflection coatings in order to simplify the cavity design, and further scale the output power. The utilization of thermally insensitive orientations will require the knowledge of the thermo-optic coefficients. Special coatings of the cavity mirrors are expected to allow the generation of even shorter mode-locked pulses with Yb:KLuW. The search for suitable passive elements with saturable absorption for Q-switching and mode-locking in the 2- μm spectral range will also continue.

ACKNOWLEDGMENTS

This work was supported by the EU Project DT-CRYS (NMP3-CT-2003-505580). We also acknowledge financial support from the Spanish Government by the Projects MAT2005-06354-C03-02, MAT2004-20471-E and CIT-020400-2005-14, and from the Catalan Government by the Project 2005SGR658. X. Mateos acknowledges financial support from the Secretaria de Estado de Educacion y Universidades of Spain and from the Fondo Social Europeo. We thank C. Kränkel and K. Petermann (Hamburg University, Germany) for the pinhole measurements of the lifetimes, M. Galan and G. Viera (Monocrom S.L., Spain) for the AlGaAs diode laser used for pumping near 800 nm, G. Erbert (Ferdinand-Braun-Institut, Germany) for the TDL, and M. Zorn and M. Weyers (Ferdinand-Braun-Institute, Germany) for the SESAM used in the mode-locking experiments.

REFERENCES

1. P. V. Klevtsov and L. P. Kozeeva, "Synthesis and x-ray and thermal studies of potassium rare-earth tungstates, $\text{KLn}(\text{WO}_4)_2$, Ln=rare-earth element," *Sov. Phys. - Dokl.* **14**, 185-187 (1969) [transl. from *Dokl. Akad. Nauk SSSR* **185**, 571-574 (1969)].
2. A. A. Kaminskii, K. Ueda, H. E. Eichler, J. Findeisen, S. N. Bagaev, F. A. Kuznetsov, A. A. Pavlyuk, G. Boulon, F. Bourgeois, "Monoclinic tungstates $\text{K Dy}(\text{WO}_4)_2$ and $\text{K Lu}(\text{WO}_4)_2$: New $\chi^{(3)}$ -active crystals for laser Raman shifters," *Jpn. J. Appl. Phys.* **37**, L923-L926 (1998).
3. J. Hanuza and L. Macalik, "Polarized infra-red and Raman spectra of monoclinic α - $\text{KLn}(\text{WO}_4)_2$ single crystals (Ln=Sm-Lu, Y)," *Spectrochimica Acta* **43A**, 361-373 (1987).
4. A. A. Kaminskii, A. A. Pavlyuk, N. R. Agamalyan, L. I. Bobovich, A. V. Lukin, V. V. Lyubchenko, "Stimulated emission by $\text{K Lu}(\text{WO}_4)_2\text{-Er}^{3+}$ crystals at room temperature," *Inorg. Mater.* **15**, 1182-1183 (1979) [transl. from *Izv. Akad. Nauk SSSR, Neorganicheskie Materialy* **15**, 1496-1497 (1979)].
5. T. S. Avsievich, V. N. Verenik, A. A. Pavlyuk, R. A. Puko, A. P. Shkadarevich, V. D. Yarzhemkovskii, "Kinetics of the luminescence of the Ho^{3+} ion $\text{K A}''(\text{WO}_4)_2$ crystals," *J. Appl. Spectr.* **44**, 248-251 (1986) [transl. from *Zhurnal Prikladnoi Spektroskopii* **44**, 407-410 (1986)].
6. A. A. Kaminskii, A. G. Petrosyan, V. A. Fedorov, S. E. Sarkisov, V. V. Ryabchenkov, A. A. Pavlyuk, V. V. Lyubchenko, I. V. Mochalov, "Two-micron stimulated emission by crystals with Ho^{3+} ions, based on the transition $^5I_7 \rightarrow ^5I_8$," *Sov. Phys. - Dokl.* **26**, 846-848 (1981) [transl. from *Dokl. Akad. Nauk SSSR* **260**, 64-67 (1981)].
7. A. A. Kaminskii, A. A. Pavlyuk, N. R. Agamalyan, S. E. Sarkisov, L. I. Bobovich, A. V. Lukin, V. V. Lyubchenko, "Stimulated radiation of Nd^{3+} and Ho^{3+} ions in monoclinic $\text{K Lu}(\text{WO}_4)_2$ crystals at room temperature," *Inorg. Mater.* **15**, 1649 (1979) [transl. from *Izv. Akad. Nauk SSSR, Neorganicheskie Materialy* **15**, 2092 (1979)].
8. A. A. Kaminskii, N. R. Agamalyan, A. A. Pavlyuk, L. I. Bobovich, V. V. Lyubchenko, "Preparation and luminescence-generation properties of $\text{K Lu}(\text{WO}_4)_2\text{-Nd}^{3+}$," *Inorg. Mater.* **19**, 885-894 (1983) [transl. from *Izv. Akad. Nauk SSSR, Neorganicheskie Materialy* **19**, 982-991 (1983)].
9. A. A. Kaminskii, A. I. Bodretsova, A. G. Petrosyan, A. A. Pavlyuk, "New quasi-CW pyrotechnically pumped crystal lasers," *Sov. J. Quantum Electron.* **13**, 975-976 (1983) [transl. from *Kvantovaya Elektron. (Moscow)* **10**, 1493-1494 (1983)].
10. A. A. Kaminskii, H. R. Verdun, W. Koechner, F. A. Kuznetsov, A. A. Pavlyuk, "Efficient single-mode cw lasers based on monoclinic double potassium-(rare earth) tungstenate crystals containing Nd^{3+} ions with semiconductor-laser pumping," *Sov. J. Quantum Electron.* **22**, 875-877 (1992) [transl. from *Kvantovaya Elektron. (Moscow)* **19**, 941-943 (1992)].
11. L. Tang, Z. Lin, Z. Hu, G. Wang, "Growth and spectral properties of $\text{Nd}^{3+}:\text{K Lu}(\text{WO}_4)_2$ crystal," *J. Cryst. Growth* **277**, 228-232 (2005).
12. L. Tang and G. Wang, "Spectral parameters of Nd^{3+} ion in $\text{Nd}^{3+}:\text{K Lu}(\text{WO}_4)_2$ crystal," *Chinese J. Struct. Chem.* **23**, 383-386 (2005).
13. J. Zhang, J. Wang, H. Zhang, F. Xu, Z. Wang, Z. Shao, H. Zhao, Y. Wang, "Growth and diode-pumped CW lasing of $\text{Nd}:\text{K Lu}(\text{WO}_4)_2$," *J. Cryst. Growth* **284**, 108-111 (2005).
14. L. I. Yudanov, O. G. Potapova, A. A. Pavlyuk, "Phase diagram of the system $\text{K Lu}(\text{WO}_4)_2\text{-K Nd}(\text{WO}_4)_2$ and growth of $\text{K Lu}(\text{WO}_4)_2$ single crystals," *Inorg. Mater.* **23**, 1657-1660 (1987) [transl. from *Izv. Akad. Nauk SSSR, Neorganicheskie Materialy* **23**, 1884-1887 (1987)].
15. P. V. Klevtsov, L. P. Kozeeva, L. Yu. Kharchenko, "Study of the crystallization and polymorphism of double potassium and trivalent metal tungstates, $\text{KR}(\text{WO}_4)_2$," *Sov. Phys. Crystallogr.* **20**, 732-735 (1975) [transl. from *Kristallografiya* **20**, 1210-1215 (1975)].
16. K. Wang, J. Zhang, J. Wang, W. Yu, H. Zhang, Z. Wang, Z. Shao, "Spectral and luminescent properties of trivalent samarium ions in $\text{K Lu}(\text{WO}_4)_2$ crystals," *Mat. Res. Bull.* **41**, 1695-1700 (2006).
17. J. Wang, H. Zhang, Z. Wang, W. Ge, J. Zhang, M. Jiang, "Growth, properties and Raman shift laser in tungstate crystals," *J. Cryst. Growth* **292**, 377-380 (2006).
18. H. Zhao, J. Wang, J. Li, J. Zhang, H. Zhang, M. Jiang, "Growth, optical and thermal properties of $\text{Yb, Tm}:\text{K Lu}(\text{WO}_4)_2$," *J. Cryst. Growth* **293**, 223-227 (2006).
19. X. Mateos, V. Petrov, M. Aguilo, R. M. Sole, J. Gavaldà, J. Massons, F. Diaz, U. Griebner, "Continuous-wave laser oscillation of Yb^{3+} in monoclinic $\text{K Lu}(\text{WO}_4)_2$," *IEEE J. Quantum Electron.* **40**, 1056-1059 (2004).

-
20. X. Mateos, R. Sole, Jna. Gavalda, M. Aguilo, J. Massons, F. Diaz, V. Petrov, U. Griebner, "Crystal growth, spectroscopic studies and laser operation of Yb³⁺-doped potassium lutetium tungstate," *Opt. Mat.* **28**, 519-523 (2006).
 21. J. Liu, U. Griebner, V. Petrov, H. Zhang, J. Zhang, J. Wang, "Efficient continuous-wave and Q-switched operation of a diode-pumped Yb:KLu(WO₄)₂ laser with self-Raman conversion," *Opt. Lett.* **30**, 2427-2429 (2005).
 22. U. Griebner, S. Rivier, V. Petrov, M. Zorn, G. Erbert, M. Weyers, X. Mateos, M. Aguilo, J. Massons, F. Diaz, "Passively mode-locked Yb:KLu(WO₄)₂ oscillators," *Opt. Exp.* **13**, 3465-3470 (2005).
 23. U. Griebner, J. Liu, S. Rivier, A. Aznar, R. Grunwald, R. M. Sole, M. Aguilo, F. Diaz, V. Petrov, "Laser operation of epitaxially grown Yb:KLu(WO₄)₂-KLu(WO₄)₂ composites with monoclinic crystalline structure," *IEEE J. Quantum Electron.* **41**, 408-414 (2005).
 24. V. Petrov, S. Rivier, U. Griebner, J. Liu, X. Mateos, A. Aznar, R. Sole, M. Aguilo, F. Diaz, "Epitaxially grown Yb:KLu(WO₄)₂ composites for continuous-wave and mode-locked lasers in the 1 μm spectral range," *J. Non-Cryst. Sol.* **352**, 2367-2370 (2006).
 25. S. Rivier, X. Mateos, V. Petrov, U. Griebner, A. Aznar, O. Silvestre, R. Sole, M. Aguilo, F. Diaz, M. Zorn, M. Weyers, "Mode-locked laser operation of epitaxially grown Yb:KLu(WO₄)₂ composites," *Opt. Lett.* **30**, 2484-2486 (2005).
 26. V. Petrov, J. Liu, M. Galan, G. Viera, C. Pujol, U. Griebner, M. Aguilo, F. Diaz, "Efficient diode-pumped cw Tm:KLu(WO₄)₂ laser," *Proc. SPIE* **6216**, 161-170 (2006).
 27. X. Mateos, V. Petrov, J. Liu, M. C. Pujol, U. Griebner, M. Aguilo, F. Diaz, M. Galan, G. Viera, "Efficient 2-μm continuous-wave laser oscillation of Tm³⁺:KLu(WO₄)₂," *IEEE J. Quantum Electron.* **42**, 1008-1015 (2006).
 28. O. Silvestre, M. C. Pujol, M. Aguilo, F. Diaz, X. Mateos, V. Petrov, U. Griebner, "CW laser operation of KLu_{0.945}Tm_{0.055}(WO₄)₂/KLu(WO₄)₂ epilayers near 2-μm," *IEEE J. Quantum Electron.* (2006), in press.
 29. P. V. Klevtsov, L. P. Kozeeva, L. Lu. Kharchenko, A. A. Pavlyuk, "Polymorphism of KY(WO₄)₂ and isostructural potassium-rare earth tungstates," *Sov. Phys. Crystallogr.* **19**, 342-346 (1974) [transl. from *Kristallografiya* **19**, 552-559 (1974)].
 30. R. Sole, V. Nikolov, X. Ruiz, Jna. Gavalda, X. Solans, M. Aguilo, F. Diaz, "Growth of β-KGd_{1-x}Nd_x(WO₄)₂ single crystals in K₂W₂O₇ solvents," *J. Cryst. Growth*, **169**, 600-603 (1996).
 31. M. C. Pujol, X. Mateos, A. Aznar, X. Solans, S. Surinach, J. Massons, F. Diaz, M. Aguilo, "Structural redermination, thermal expansion and refractive indices of KLu(WO₄)₂," *J. Appl. Cryst.* **39**, 230-236 (2006).
 32. A. Aznar, O. Silvestre, M. C. Pujol, R. Sole, M. Aguilo, F. Diaz, "Liquid-phase epitaxy crystal growth of monoclinic KLu_{1-x}Yb_x(WO₄)₂/KLu(WO₄)₂ layers," *Crystal Growth & Design* **6**, 1781-1787 (2006).
 33. K. Wang, J. Zhang, J. Wang, W. Yu, H. Zhang, Z. Wang, X. Wang, M. Ba, "Predicted and real habits of flux grown potassium lutetium tungstate single crystals," *Crystal Growth & Design* **5**, 1555-1558 (2005).
 34. K. Wang, J. Zhang, J. Wang, W. Yu, H. Zhang, Z. Wang, "Periodic transition of microcrystals on the host (110) face of KLu(WO₄)₂ crystals," *J. Appl. Cryst.* **38**, 975-978 (2005).
 35. K. Wang, J. Zhang, J. Wang, W. Yu, H. Zhang, Z. Wang, M. Ba, "Investigation of growth mechanisms of TSS-grown KLu(WO₄)₂ crystals by atomic force microscopy," *Opt. Mat.* (2006), in press.
 36. J. Zhang, J. Wang, K. Wang, W. Yu, H. Zhang, Z. Wang, X. Wang, M. Ba, "Growth and structure of monoclinic KLu(WO₄)₂ crystals," *J. Cryst. Growth* **292**, 373-376 (2006).
 37. O. Silvestre, M. C. Pujol, M. Rico, F. Güell, M. Aguilo, F. Diaz, "Thulium doped monoclinic KLu(WO₄)₂ single crystals: growth and spectroscopy," *Appl. Phys. B* (2006), submitted.
 38. Y. Jiang, K. Wang, X. Wang, C. Jia, J. Zhang, J. Wang, H. Ma, R. Nie, D. Shen, "Optical waveguide formed in Yb:KLu(WO₄)₂ crystal by 6.0 MeV O⁺ implantation," *Chin. Phys. Lett.* **23**, 922-924 (2006).
 39. M. C. Pujol, M. A. Bursukova, F. Güell, X. Mateos, R. Solé, Jna. Gavalda, M. Aguiló, J. Massons, F. Diaz, P. Klopp, U. Griebner, V. Petrov, "Growth, optical characterization, and laser operation of a stoichiometric crystal KYb(WO₄)₂," *Phys. Rev. B* **65**, 165121-1-11 (2002).
 40. J. Zhang, K. Wang, J. Wang, H. Zhang, W. Yu, X. Wang, Z. Wang, Q. Lu, M. Ba, D. G. Ran, Z. C. Ling, H. R. Xia, "Anisotropic thermal properties of monoclinic Yb:KLu(WO₄)₂ crystals," *Appl. Phys. Lett.* **87**, 061104-1-3 (2005).
 41. K. Wang, J. Zhang, J. Wang, H. Zhang, Z. Wang, W. Yu, X. Wang, Q. Lu, M. Ba, "Anisotropic thermal expansion of monoclinic potassium lutetium tungstate single crystals," *J. Appl. Phys.* **98**, 046101-1-3 (2005).
 42. Z. C. Ling, H. R. Xia, S. Q. Sun, D. G. Ran, F. Q. Liu, P. Zhao, C. Y. Gao, J. X. Zhang, J. Y. Wang, "Lattice vibration and thermal diffusion of Yb doped KLu(WO₄)₂ single crystal," *J. Appl. Phys.* **100**, 043522-1-6 (2006).